JOURNAL OF MATERIALS SCIENCE 27 (1992) 1937–1946

Operating regimes for laser surface engineering of ceramics

K. MOHAMMED JASIM*, R. D. RAWLINGS, D. R. F. WEST
Department of Materials, Imperial College of Science, Technology and Medicine, Exhibition Road, London SW7 2BP, UK

Results obtained with CO_2 lasers on the effect of processing parameters were used to determine the operating regimes for laser sealing and laser cladding of ceramics with particular reference to zirconias. The specific energy required for laser cladding is higher by at least two orders of magnitude than that required for laser sealing of plasma-sprayed ceramics at a given power density.

1. Introduction

The availability of high-power lasers in recent years has led to a range of applications in materials processing such as cutting, welding, drilling and surface engineering; the latter includes surface hardening, melting, alloying, and cladding. Much research has been carried out on a wide range of laser surface treatments of metallic materials; in contrast there is a relative dearth of information on the laser surface processing of ceramics.

The temperature rise during laser treatments depends on two factors. Firstly, the properties of the material (e.g. absorptivity and thermal diffusivity) and secondly the laser parameters such as power, P, beam diameter, d, wavelength, λ, and interaction time, t, [1]. Heat transfer rapidly occurs to a distance called the thermal diffusion length which is given by $(2Dt)^{0.5}$, where t is the interaction time and D is the thermal diffusivity which equals $(k/\rho c)$, where k is thermal conductivity, ρ is density and c is specific heat [1]. Combined laser parameters such as power density $P_A = 4P/\pi d^2$ (W mm^{-2}), and specific energy, $S = P/dV$ (J mm^{-2}), where V is the traverse speed of the component, are frequently employed to specify the laser processing conditions. Power density/traverse speed, $P_v = 4P/\pi d^2 V$ (J mm^{-3}) has also been used [2]. Different values for these parameters result in one or more of the following effects illustrated in Fig. 1; for metals these occur at the following power density values [3]:

1. Heating without melting, at power density $\sim < 10^2$ W mm^{-2}.
2. Melting, at power density $\sim 10^2$–10^4 W mm^{-2}.
3. Evaporation, at power density $\sim 10^4$–10^6 W mm^{-2}.
4. Plasma formation, at power density $\sim > 10^6$ W mm^{-2}.

Many techniques have been used to enhance the surface properties of bulk materials either by surface heat treatment or by applying coating layers [4]. Recently laser beams have been used successfully as an effective tool for a wide range of surface treatments [5]. The absorptivity is considered to be the single most important material property determining the efficiency of laser processing. In some materials, such as bulk ceramics and plasma-sprayed ceramic layers, the absorptivity is very high; however, in metals it is low.

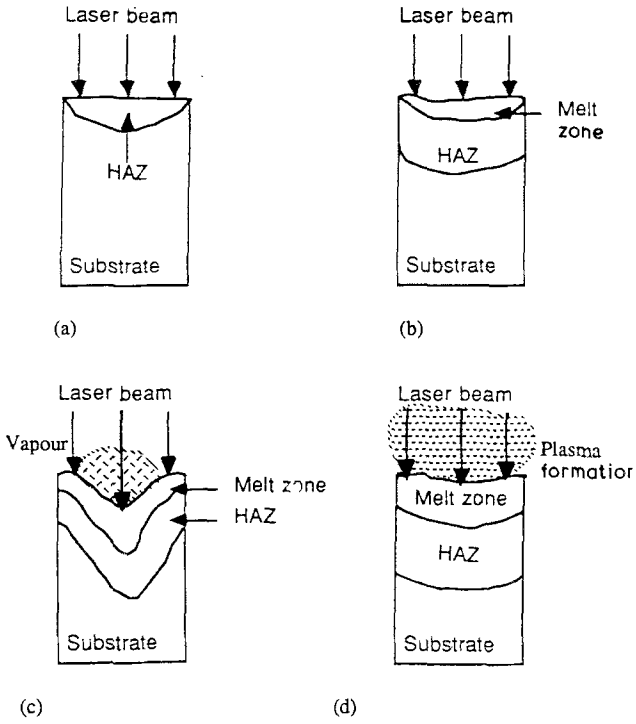

Figure 1 Schematic diagrams of physical processes occurring when a high-power laser strikes an absorbing surface. (a) Heating, (b) melting, (c) vaporization, (d) plasma formation.

Generally, wide beams of as uniform intensity as possible are preferred for use in laser surface treatment in order to obtain a uniform depth of melting, alloying or cladding and to cover a large area by multiple, partially overlapping tracks. High power densities, $\sim > 10^4$ W mm^{-2}, are required for welding, cutting

* On leave from Scientific Research Council, Baghdad. *Present address*: PO Box 9225, Kadhimiya, Baghdad, Iraq.

and drilling of metals while lower power densities, $\sim 10^2$–10^4 W mm^{-2}, are more suitable for laser surface treatments.

The results presented in this paper establish the laser processing conditions for cladding of zirconia-based ceramics on to a metal substrate and for modification by surface sealing (melting) of a plasma-sprayed ceramic coating on a metal substrate. Details of all the results are not reported here but most can be found in previous publications [6–11]; in this paper selected results are presented to illustrate important trends.

2. Experimental procedure

The plasma-sprayed layers for laser sealing were produced commercially using an automatic robot spraying coating system. All the sprayed layers were zirconia based (Table I), $\sim$ 200–700 μm thickness and were deposited on to mild steel or Nimomic 75 substrates. For laser processing, the plasma-sprayed samples were fixed into a jig which was clamped to a x–y table. Most runs were carried out with an effective shrouding system involving a flow of argon to protect the sealed layer from the atmosphere; a few experiments were performed without shrouding gas or with partial shrouding [6, 7]. Single and partially overlapped tracks were produced.

In the laser cladding, the cladding power was blown through a 3 mm diameter copper tube by argon gas at a high volume flow into the laser-generated melt pool. Powder at the desired feed rate was continuously fed through the laser beam on to the sample which was traversed at a set speed within the range 1–40 mm s^{-1}. Table II summarizes the laser parameters used for both laser sealing and cladding.

The upper surfaces of the clad and sealed samples were examined by scanning electron microscopy without any prior grinding or polishing. Surface roughness was quantified by means of centre line average (CLA) values obtained by a Talysurf. The samples were then carefully cut, ground and polished in order to examine the transverse section.

TABLE I Ceramic materials studied

Laser sealing	Laser cladding
8 wt% yttria-stabilized zirconia	8.5 wt% yttria-stabilized zirconia
8.5 wt% yttria-stabilized zirconia	20 wt% yttria-stabilized zirconia
20 wt% yttria-stabilized zirconia	Pure zirconia
6 wt% calcia-stabilized zirconia	Pure alumina
30 wt% calcia-stabilized zirconia	Pure magnesia
25 wt% ceria-stabilized zirconia	95 wt% (8.5 wt% YSZ) + 5 wt% alumina
90 wt% (8.5 wt% YSZ) + 10 wt% alumina	90 wt% (8.5 wt% YSZ) + 10 wt% alumina

TABLE II Laser parameters studied

Parameter	Laser sealing	Laser cladding
Power (kW)	0.4–2.2	1–2.2
Traverse speed (mm s^{-1})	5–400	1–40
Beam diameter (mm)	0.4–10	3–8
Specific energy (J mm^{-2})	0.27–88	15–230
Power density (W mm^{-2})	16–6300	20–315

3. Results

The results presented are for single tracks. However, it was found that the characteristics of the laser-processed surface were not significantly changed when multiple partially overlapped tracks were produced. Thus the general trends and conclusions given in this paper may be considered to be valid for both single and partially overlapped tracks.

3.1 Laser sealing

The objective of sealing is to produce a layer, essentially free from porosity on the surface of the plasma-sprayed coating. The plasma-sprayed material has some desirable characteristics and it is not the intention to completely melt it. The depth of the sealed layer obtained with the various combination of laser parameters studied, ranged from effectively zero to greater than the thickness of the plasma coating. However, typically, in the present work, a depth of sealing of $\sim$ 20–100 μm was aimed for.

Fig. 2 shows the relationship between traverse speed and depth of sealing at different powers for 8.5 wt% yttria-stabilized zirconia; similar plots were obtained from the other ceramics investigated. The following observations can be made from this Figure.

(i) The depth of sealing is decreased with increasing traverse speed and decreasing power.

(ii) At 0.8 and 1 kW, the decrease in depth of sealing with increasing speed is not as marked as at the highest power of 1.4 kW. The very shallow depth of sealing of $\sim$ 10 μm obtained at low power and high speed, i.e. at low specific energy, corresponds to partial sealing (only local regions of melting) and is, therefore, unacceptable. Figs 3 and 4 show scanning electron micrographs of the depth of sealing at 0.8 and 1 kW at different speeds.

(iii) At 1.4 kW and low speeds, < 30 mm s^{-1}, the depth of sealing was equal to or greater than the thickness of the plasma-sprayed layer (i.e. complete

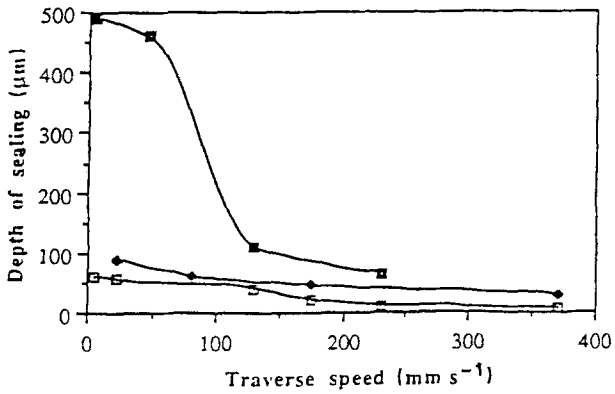

Figure 2 The relationship between depth of sealing and traverse speed (8.5 wt % YSZ). Plasma sprayed thickness was $\sim$ 500 and 200 μm for (■ 1.4 kW and (◆/□) 1.0/0.8 kW, respectively.

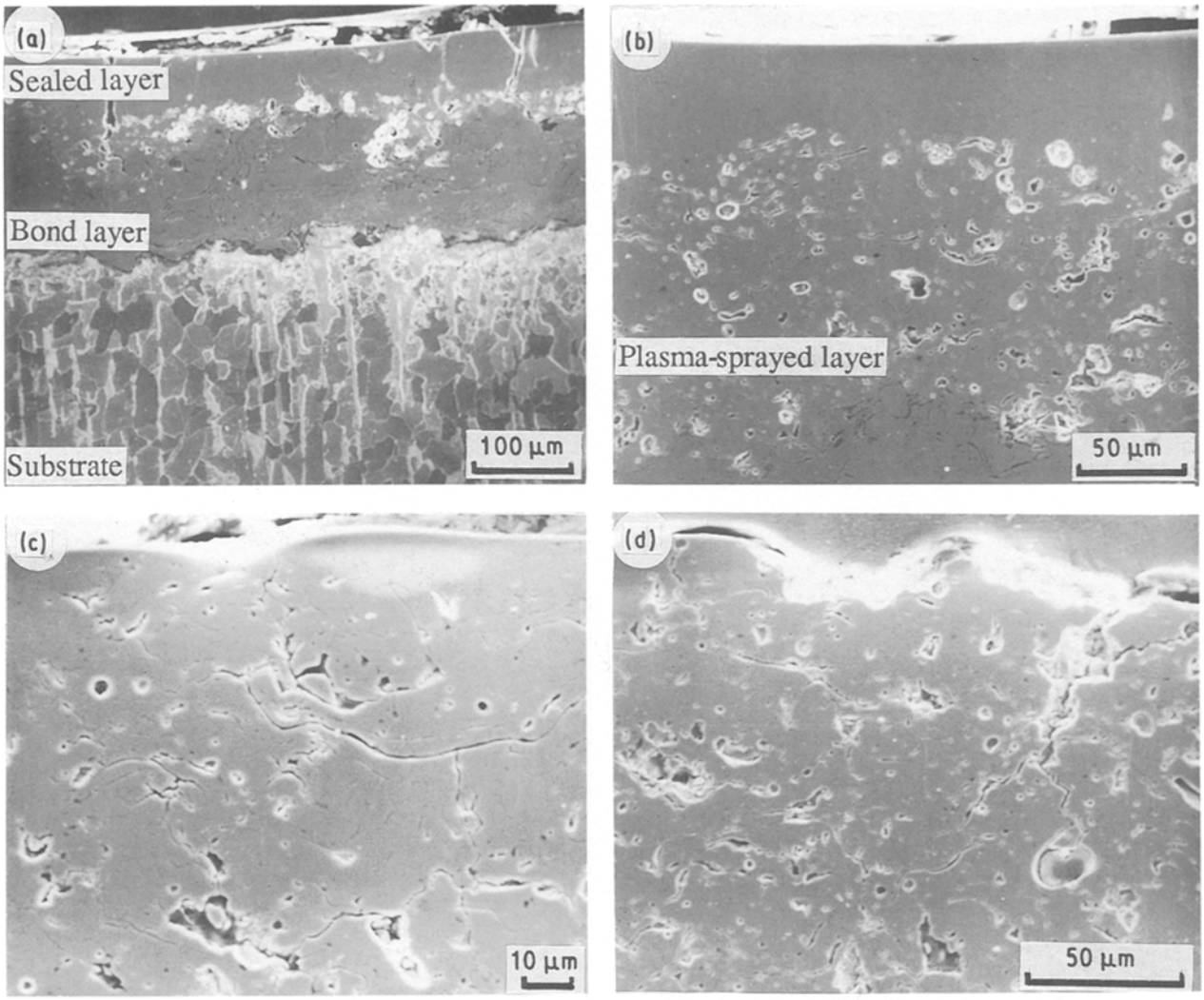

Figure 3 Transverse sections of 8.5 wt % YSZ sealed layers showing the depth of sealing at different traverse speeds; 0.8 kW laser power, 5 mm beam diameter and 200 μm plasma-sprayed thickness. (a) 5.3 mm s^{-1}, (b) 22 mm s^{-1}, (c) 175 mm s^{-1}, (d) 230 mm s^{-1}.

melting of plasma-sprayed or plasma-sprayed plus bond layer and part of the substrate). For example, at the lowest speed used, 5.3 mm s^{-1}, melting of the bond layer and part of the substrate occurred (Fig. 5a–d). With increase in the speed to 22 mm s^{-1}, complete melting of the sprayed layer was observed but the bond layer had not melted. Further increase in traverse speed sharply decreases the depth of sealing to an acceptable value.

The relationship between the depth of sealing within the acceptable limits and specific energy at low powers is given by a power law

$$D_s = 0.04\ S^{0.4} \quad (1)$$

where D_S is the depth of sealing (mm) and S is the specific energy (J mm^{-2}). This equation, with S raised to the power 0.4, was found to apply approximately for all the materials investigated, except 30 wt% CaSZ. In this depth range the depth of sealing is conduction limited and as such, to the first approximation, D_s may be considered to be proportional to $t^{0.5}$ where t is the interaction time; but t is inversely proportional to speed and hence D_s should vary as $S^{0.5}$, which is in reasonable agreement with the experimental data.

Examination of cross-sections revealed that the surface of a laser track was often concave, the depth of the concavity at the centre of the track being a function of the laser conditions and the ceramic. A typical relationship between the depth of concavity and traverse speed under conditions of effective shrouding is shown in Fig. 6. As discussed previously, at 1.4 kW and at low speed, the depth of sealing is greater than that of the original plasma-sprayed thickness and in these circumstances the depth of concavity is negative (i.e. surface hump rather than a concavity) (see Fig. 5a). The depth of concavity then becomes approximately constant at high speeds at a low value (in the range $\sim$ 0–20 μm). At low powers (0.8 and 1 kW), the depth of concavity decreases rapidly with increasing speed and reaches values of less than 20 μm at power density/traverse speed of ~ 0.28 J mm^{-3} (180 mm s^{-1} traverse speed). The depth of the sealing and the depth of the concavity were also a function of the atmosphere during laser processing. Sealed layers produced at slow speeds and high powers, i.e. 1.2–1.7 kW, exhibited a smaller depth of sealing, but a larger depth of concavity, with shrouding gas than without shrouding. At high speeds the depths of sealing and concavity were effectively independent of atmosphere.

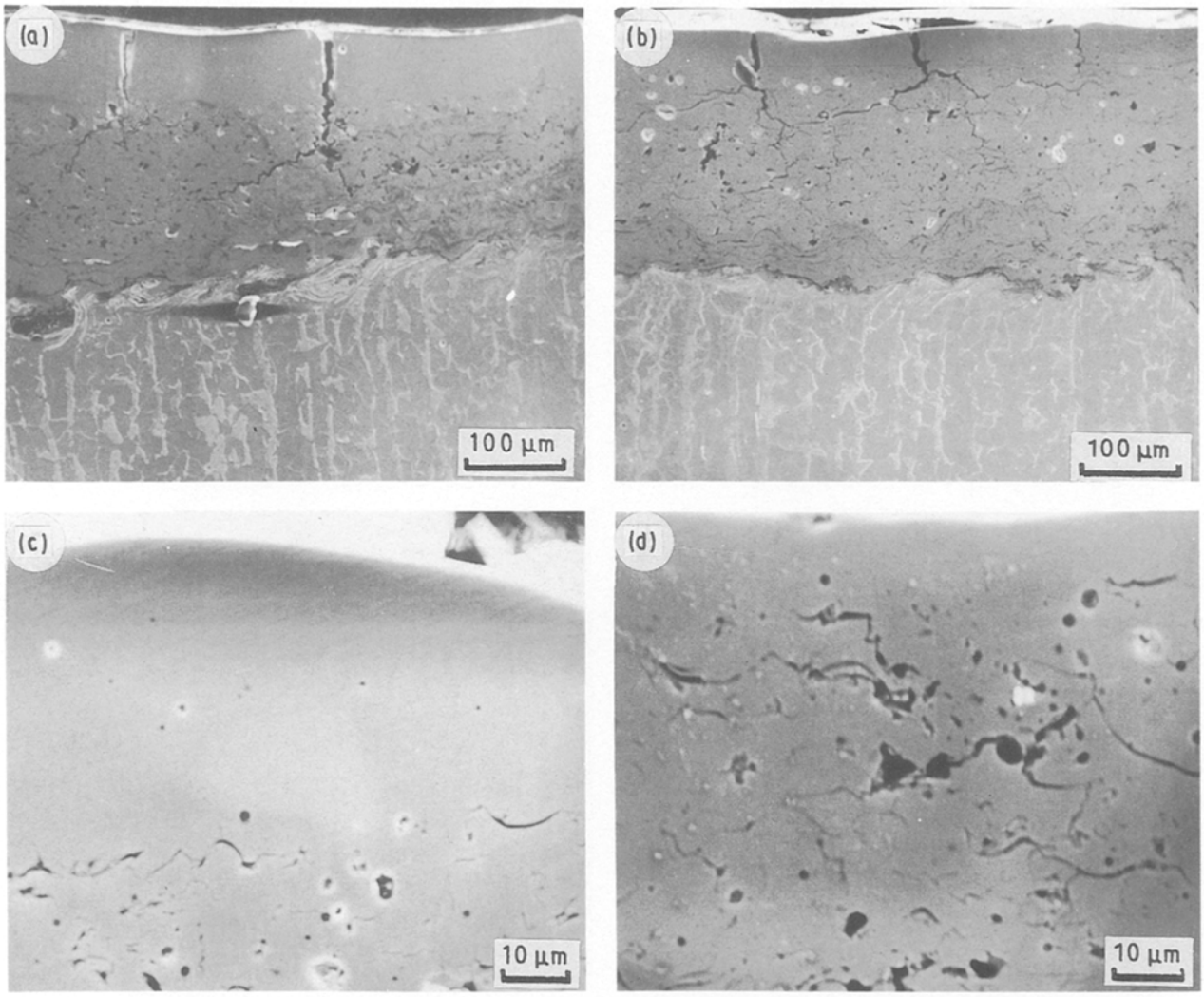

Figure 4 Transverse sections of 8.5 wt % YSZ sealed layers showing the depth of sealing at different traverse speed; 1.0 kW laser power, 5 mm beam diameter and 200 μm plasma-sprayed thickness. (a) 22 mm s^{-1}, (b) 82 mm s^{-1}, (c) 175 mm s^{-1}, (d) 370 mm s^{-1}.

Fig. 7 shows the typical plan view and transverse section of plasma-sprayed material; the ceramic layer contains open and closed porosity, together with cracks. An average CLA roughness of ~ 5 μm was found for all plasma-sprayed materials investigated. SEM observations of all sealed layers produced with or without shrouding gas showed the presence of network cracking and shallow depressions (Fig. 8). Both the crack spacing and crack width decreased with increasing traverse speed and decreasing laser power. On the other hand, the average depression size and percentage of depressions/total sealed area showed a complex relationship with traverse speed and power. It was found that these depressions can be reduced or eliminated using different processing procedures such as preheating, multipass or deep sealing (Fig. 8b, c). Higher magnification observations of the surface of the sealed layers revealed that cell-type microstructures predominated with some examples of dendritic morphologies (Fig. 9).

The benefit of using the laser beam to reduce significantly the roughness of plasma-sprayed layers is shown in Fig. 10. Measurements on the upper surface demonstrate that the sealed layers have a lower roughness compared with that of plasma-sprayed material (Fig. 11). Generally, the roughness decreased with increase in power. At acceptable sealing conditions, the roughness is low. It should be noted that a decrease in roughness is not necessarily associated with improvement in the overall quality of sealing, because roughness is also low at deep melting which often results in unsatisfactory features as far as sealing is concerned.

3.3 Laser cladding of ceramics

Fig. 12 shows the effect of traverse speed at different laser powers on the height (thickness) of the clad layer of 8.5 wt% YSZ; clad heights up to 1.5 mm were produced illustrating that laser processing is capable of coating to values similar to, or higher than, that of typical thermal barrier layers (~ 0.4 mm) produced by plasma spraying. Lower track heights can also be produced with good bonding. Although sometimes there was a small amount of porosity at the substrate/clad interface, the bonding was generally good.

There is a specific interaction time, d/V, required to melt the powder at any level of power density. For laser cladding of zirconia ceramics, the required interaction times were in the range of ~ 0.3–3 s at values of

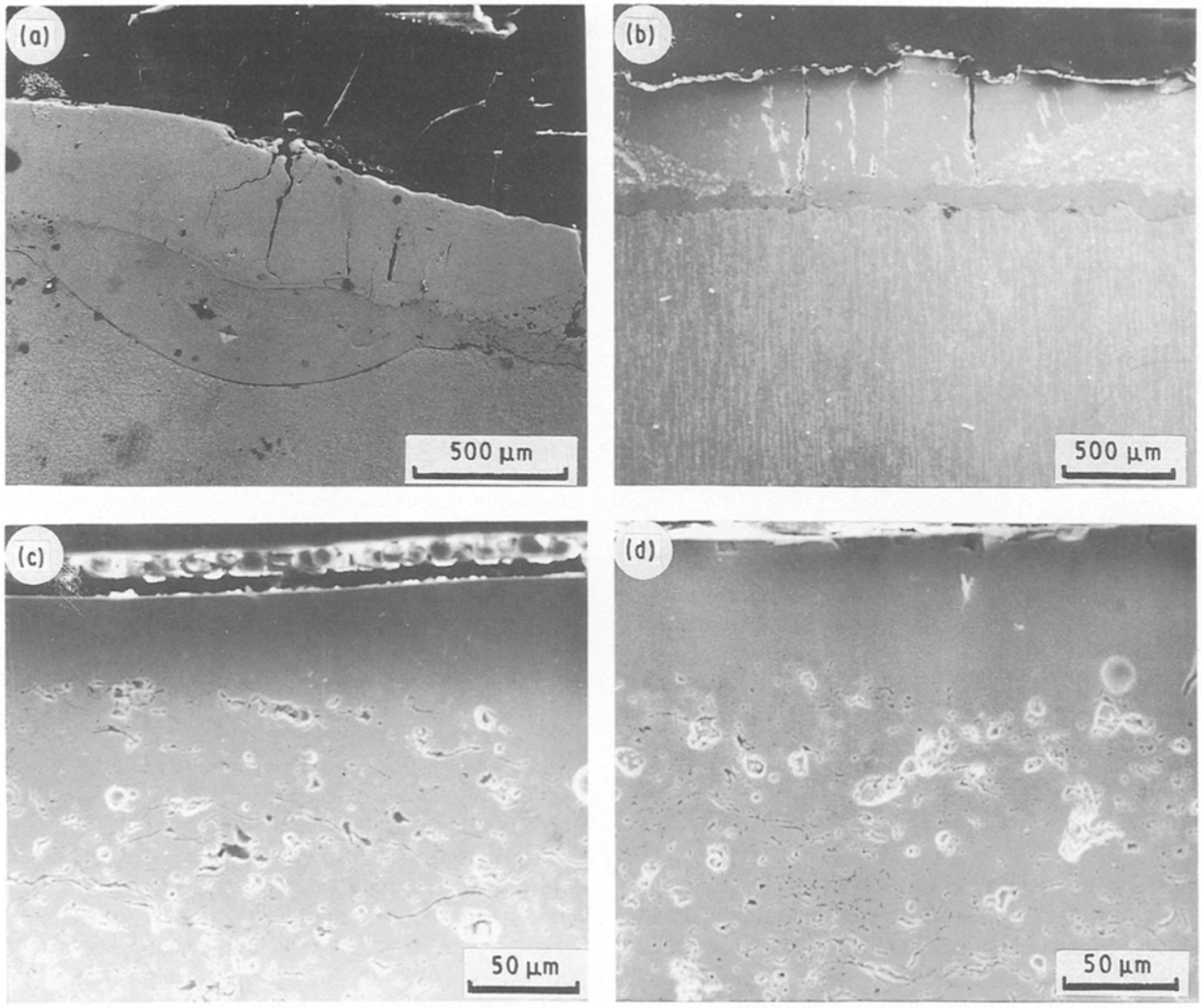

Figure 5 Transverse sections of 8.5 wt % YSZ sealed layers produced without shroud gas showing depth of sealing at different traverse speeds; 1.4 kW laser power, 5 mm beam diameter and 500 μm plasma-sprayed thickness. (a) 5.3 mm s^{-1}, showing complete sealing down to the substrate; (b) 22 mm s^{-1}, showing complete sealing down to the bond layer; (c) 130 mm s^{-1}, (d) 230 mm s^{-1}.

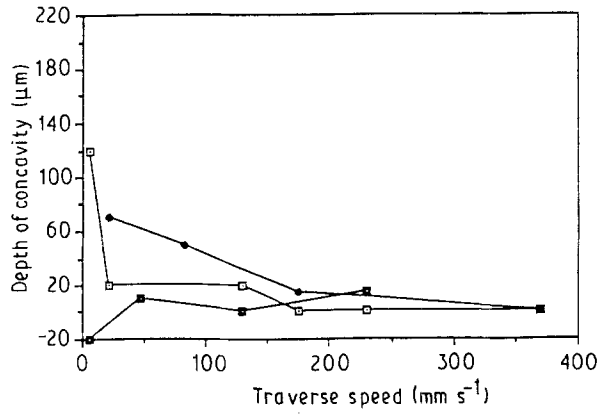

Figure 6 The relationship between depth of concavity of the sealed track and traverse speed for 8.5 wt % YSZ; (□) 0.8 kW; (◆) 1.0 kW; (■) 1.4 kW produced without shrouding gas.

power density of less than 300 W mm^{-2} and specific energy approximately 30–200 J mm^{-2}. The track height was relatively low above 5 mm s^{-1} traverse speed, i.e. short interaction times. At the high end of the speed range (20–30 mm s^{-1}) very thin cladding without complete melting was observed and at speeds above 30 mm s^{-1}, no cladding was obtained.

The clad layers produced using acceptable speeds in the range ~ 3–15 mm s^{-1} were characterized by complete melting of the powder with good bonding with the substrate (Fig. 13). Also within the optimum range, relatively smooth surfaces of CLA in the range of 1–15 μm roughness, were obtained. SEM examination of the upper surface of the clad layers did not reveal any cracking (Fig. 14). Generally, no cracks were observed in transverse section (Fig. 15) and when they were present (Fig. 13) they were probably attributable to specimen preparation. Transverse sections also showed that the level of dilution of the clad layer by localized substrate melting is less than ~ 2%. Further information regarding laser cladding of ceramics has been previously published by the authors [2, 9].

4. Discussion

The term "quality" used in this investigation in relation to laser sealing is difficult to determine fully or indeed define accurately. In the present work quality was determined by evaluating carefully all the features

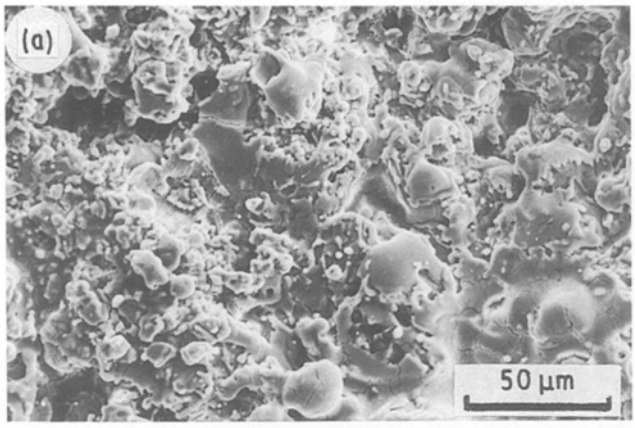

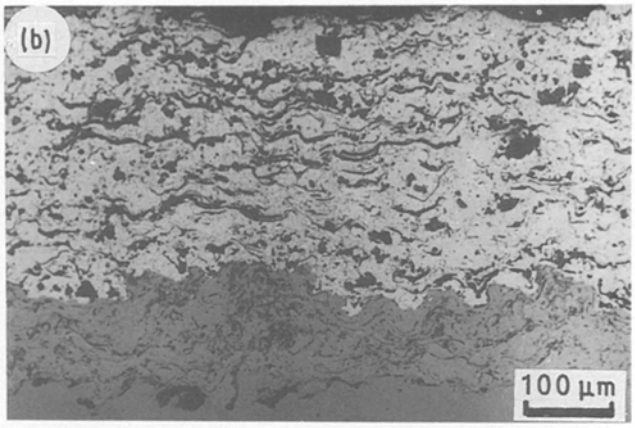

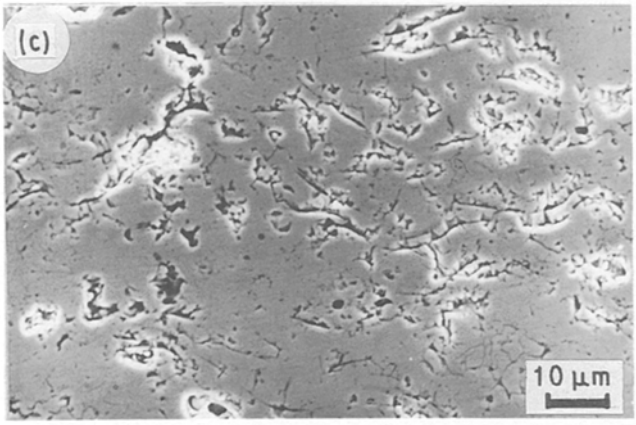

Figure 7 Scanning electron micrographs of a typical as-sprayed ceramic layer. (a) Plan view (90 wt% (8.5 wt% YSZ) ± 10 wt% alumina); (b) transverse section of (a); (c) higher magnification view of transverse section showing the presence of internal porosity and cracks (25 wt% CeSZ).

of the sealed layers as assessed from plan views and transverse sections together with surface roughness measurements. For optimum quality of sealed layers, the following features should be present which, in general, are not independent of each other:

1. The sealed layer should show complete and uniform sealing through the track and should be in the range of depth 20–100 μm for relatively thin (200–500 μm) plasma-sprayed coatings.
2. The network crack spacing [10] should be as small as possible in order to assist in relieving the stresses generated [12]. To minimize the degradation of the coating system by corrosive species, the crack width should be small (less then 5 μm for the primary cracks) and there should be only shallow penetration of the sealed layer by cracks and certainly no extension of the cracks through the plasma-sprayed layer.
3. The number of depressions and percentage area of depressions should be as low as possible and the depth and size as small as possible. The depressions will act as stress concentrators but probably more importantly they may also have different corrosion/oxidation characteristics due to concentration of harmful species in the depressions [11].

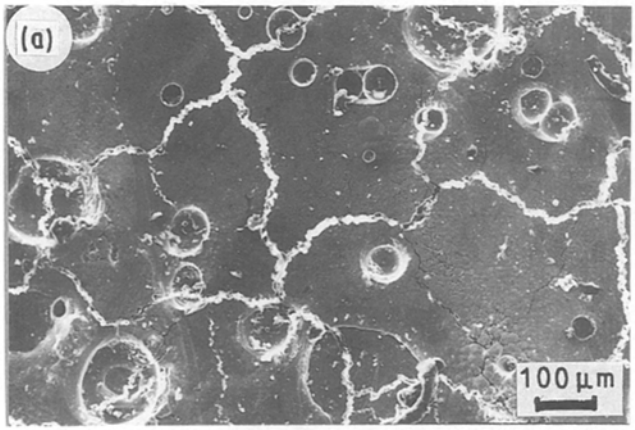

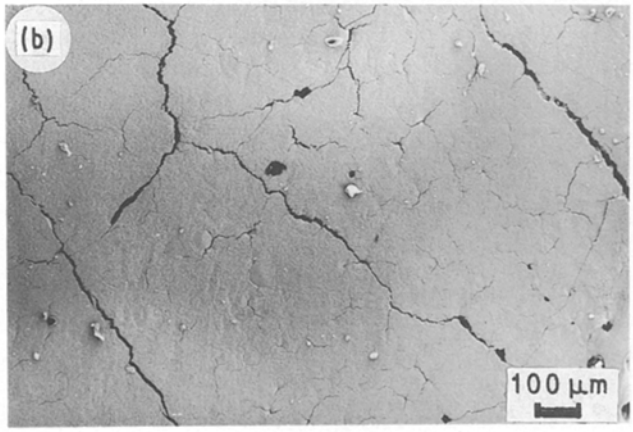

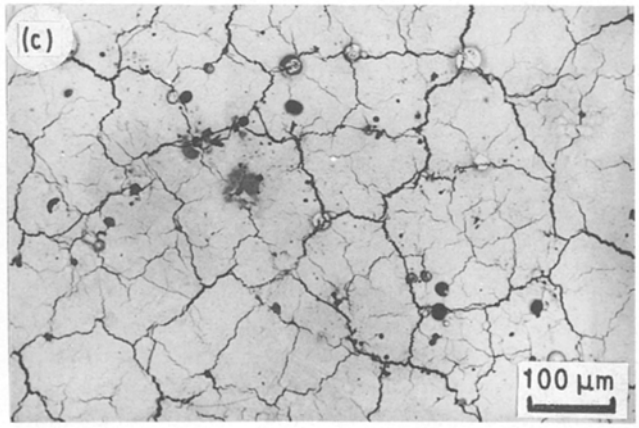

Figure 8 Typical plan views of laser sealed tracks. (a) Low magnification view showing the depressions, crack width and crack spacing (8.5 wt% YSZ); (b) deep sealing of layer showing the absence of depressions (20 wt% YSZ); (c) sealed layer produced after preheating of plasma-sprayed layer showing the absence of depressions (6 wt% YSZ).

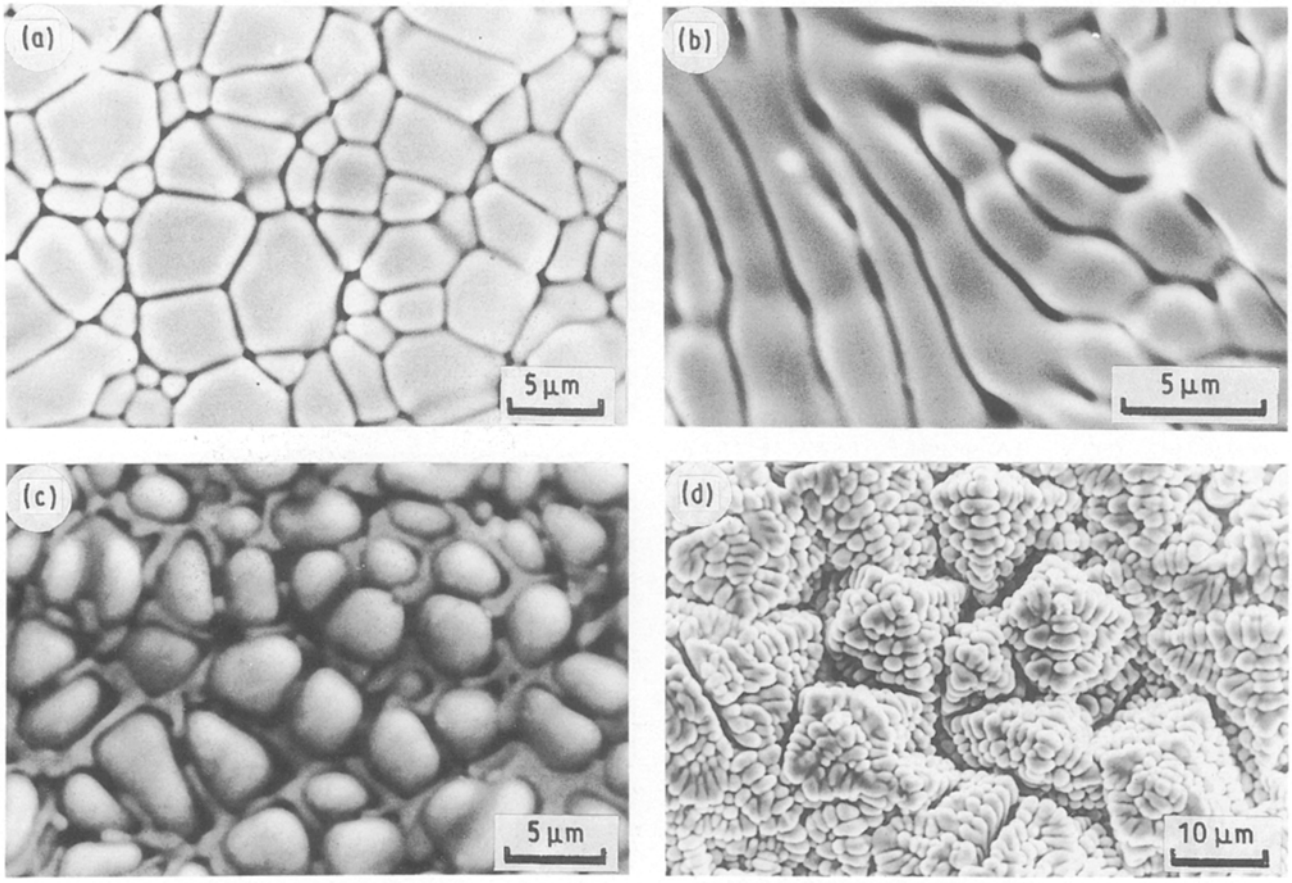

Figure 9 High-magnification plan view of the sealed layers showing the different microstructures obtained. (a) 8.5 wt% YSZ, low specific energy (cell type); (b) 8.5 wt% YSZ, high specific energy (dendritic type); (c) 30 wt% CaSZ (grains are $CaZrO_3$ and grain-boundary phase is $CaZr_4O_9$), (d) 25 wt% CeSZ (microdendritic type).

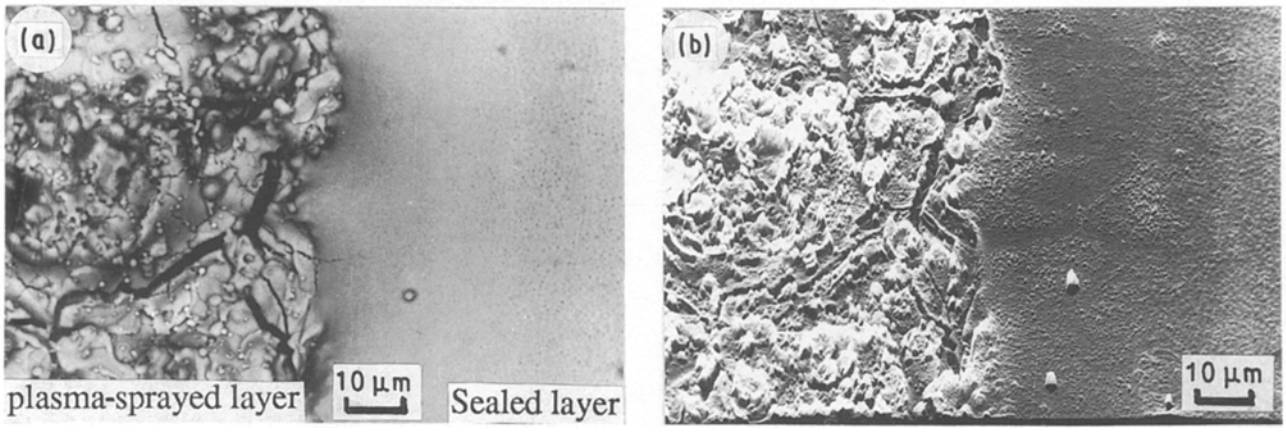

Figure 10 Typical plan view of as-sealed layer and as-sprayed layer showing the smooth surface after laser sealing. (a) Back-scattered image, (b) Y-modulated image.

4. The surface roughness, which is affected by the features of the sealed layer such as crack and depression density and morphology, should be significantly less than that of the roughness of the plasma-sprayed layer.

The effects of the different laser processing variables presented here, and elsewhere [6–11], have been correlated in terms of these four index of quality features and it was found that low values of power and interaction time, together with wide beam diameter (corresponding to low power density and specific energy) are required for laser sealing of ceramics. Data obtained were used to produce a laser-beam ceramic interaction diagram (Fig. 16). The narrow band of power density–interaction time for laser sealing indicates that ceramic materials are very sensitive to laser treatment variables. Therefore, care should be taken to control the processing conditions if good quality sealed layers are to be produced. This can be illustrated by considering an example that is on the border of

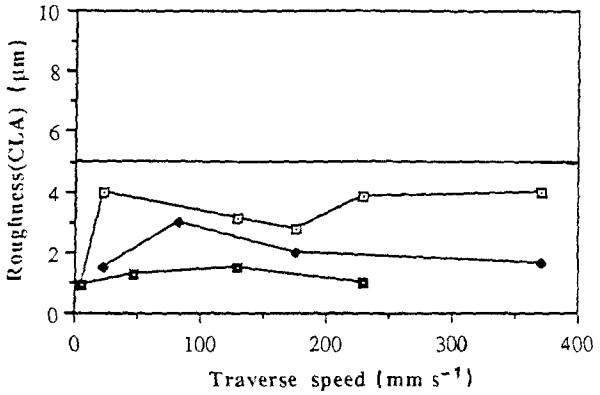

Figure 11 The variation of CLA roughness as a function of traverse speed (8.5 wt% YSZ). (——) As-sprayed, (□) 0.8 kW, (◆) 1.0 kW, (■) 1.4 kW.

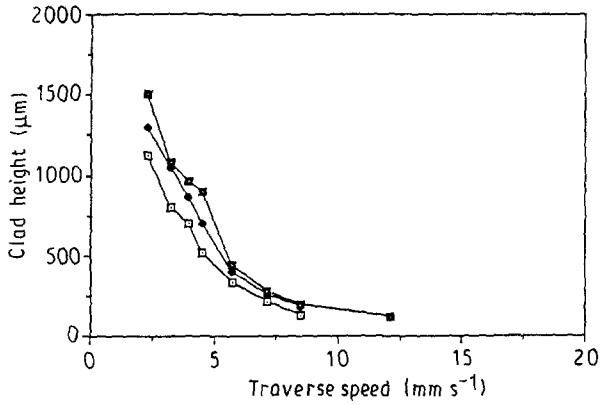

Figure 12 The relationship between clad height and traverse speed (8.5 wt% YSZ, 5 mm beam diameter, 5.7 g min^{-1} feed rate) (□) 1.2 kW, (◆) 1.4 kW, (■) 1.6 kW.

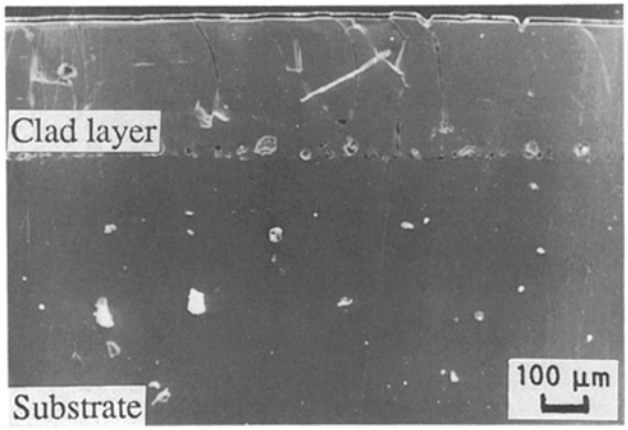

Figure 13 Longitudinal section of clad layer of 8.5 wt% YSZ on a mild steel substrate.

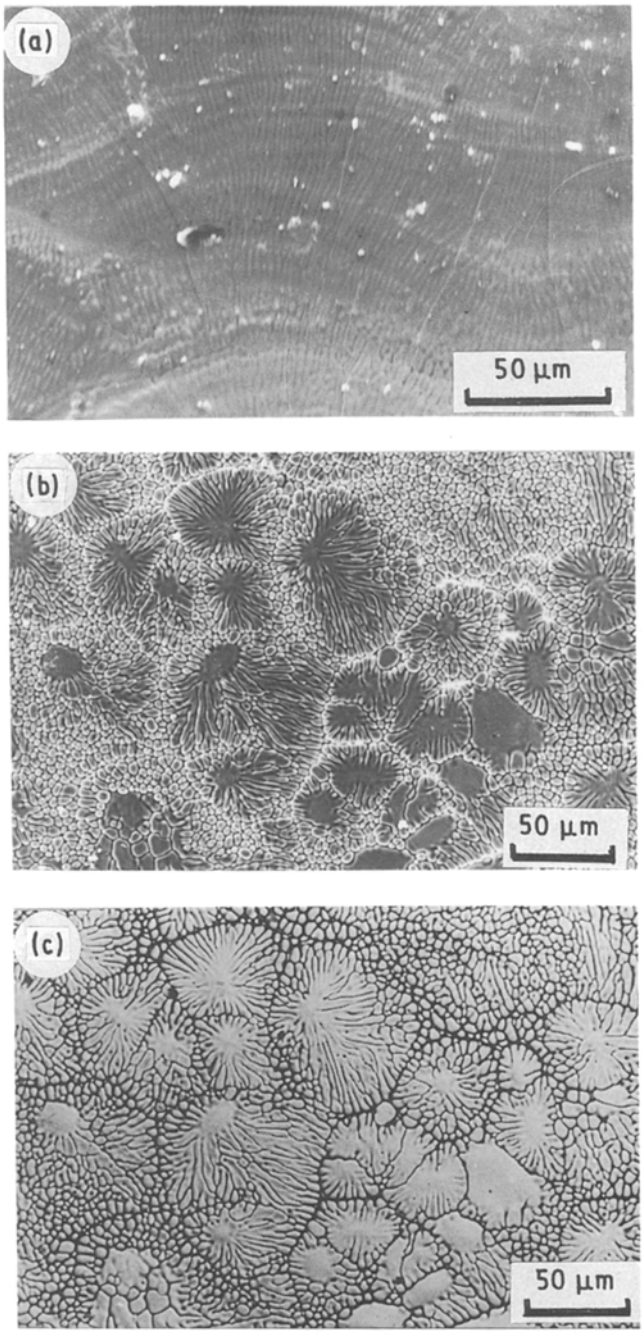

Figure 14 Scanning electron micrographs of the plan view of as-clad layers. (a) 8.5 wt% YSZ; (b) 95 wt% (8.5 wt% YSZ) + 5 wt% alumina, secondary electron image; (c) back-scattered image of (b).

the operational regime shown in Fig. 16; it was found that a small increase in the power from 0.8 to 1 kW at 5 mm beam diameter (i.e. a power density change from 41 to 51 W mm^{-2}) resulted in a drastic change in the quality. For a traverse speed of 400 mm s^{-1} and beam diameter 5 mm (interaction time equal to 12.5 ms), only partial sealing was produced at 41 W mm^{-2}, but acceptable sealing was obtained at 51 W mm^{-2} (this change corresponded to an increase in the specific energy from 0.4 to 0.5 J mm^{-2}). However, on increasing the interaction time to 25 ms at 41 W mm^{-2} power density ($S = 0.8$ J mm^{-2}), partial sealing was still observed. This example shows that 25% increase in power density allowed complete sealing to be obtained, whereas an increase in the interaction time by 100% at constant power density was insufficient to produce a change from partial to acceptable sealing (Table III). The decrease in interaction time at relatively high power densities has an important benefit in decreasing the evaporation of the plasma-sprayed layer [11].

It is concluded from the low values of power density and specific energy in Fig. 16, that a low-power laser treatment could be used effectively to obtain sealing. For example, taking the condition corresponding to

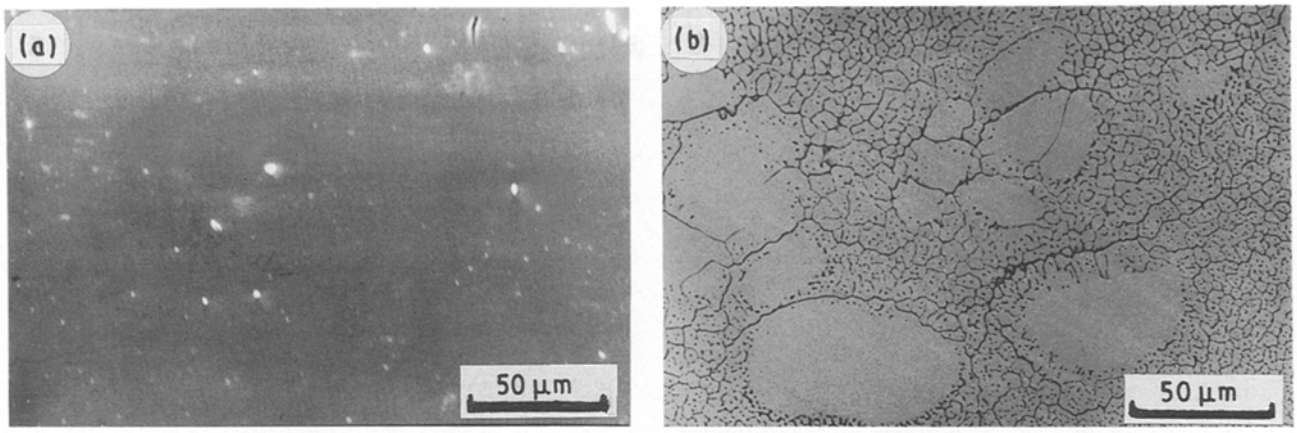

Figure 15 Scanning electron micrographs of polished transverse section of clad layers showing the absence of cracks and porosity. (a) 8.5 wt% YSZ, (b) 95 wt% (8.5 wt% YSZ) + 5 wt% alumina.

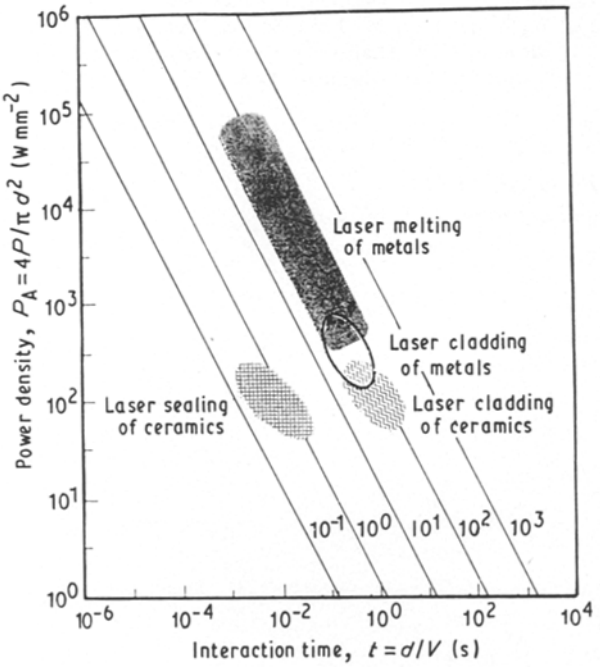

Figure 16 Operational regimes for the laser surface treatment of ceramics and metals [11]. Lines of constant specific energy values (J mm^{-2}). Note: in the present work S is taken as P/dV, as being approximately equal to $P_A t$.

TABLE III The relationship between power density, specific energy and interaction time in laser sealing of ceramic

Power density (W mm^{-2})	Specific energy (J mm^{-2})	Interaction time (ms)	Comments
41	0.4	12.5	Partial sealing
51	0.5	12.5	Complete sealing
41	0.8	25	Partial sealing
41	1	30	Complete sealing

the centre of the laser sealing regime shown in Fig. 16, namely 100 W mm^{-2} and 6 ms, it can be predicted that even 100 W power would be sufficient provided the beam was sufficiently small $\sim$ 1.2 mm.

Fig. 16 shows that longer interaction times and higher power densities are required for laser cladding compared with sealing of plasma-sprayed material. The large difference in energy required for laser cladding and sealing of ceramics is due to: (a) in laser cladding a high percentage of energy is absorbed by the high conducting metal substrate; (b) the substrate itself reflects part of the energy of the beam (for example in the extreme case of laser processing of polished steel as much as $\sim$ 95% may be reflected) [13]; (c) the formation of a plasma in laser cladding of ceramics. On the other hand, the plasma-sprayed ceramics require only low power density for sealing because they have a low reflectivity, a low thermal conductivity and only a small volume of material is involved, i.e. a small depth of sealing.

5. Conclusions

1. The operating regimes for laser sealing and laser cladding of mainly zirconia-based ceramics have been determined. Although the details will vary from one ceramic material to another, it is concluded that the general trends discussed here will provide a useful basis for laser processing of a wide range of ceramics.

2. The specific energies required for optimum laser sealing are very low compared with those required for laser melting of metals and laser cladding of ceramics. The specific energies are in the range of 0.3 –1.5 J mm^{-2} and 30–800 J mm^{-2} for laser sealing of ceramics, and melting of metals or cladding of ceramics/metals, respectively. This difference is attributed to the small volume of material being processed in laser sealing, the high efficiency of laser coupling with the plasma-sprayed layers due to low reflectivity, and the low thermal conductivity of the plasma-sprayed layers.

3. The restricted range of specific energy required to obtain a shallow depth of sealing, in the range $\sim$ 20–100 μm, of good quality, demonstrated the high dependence of the laser sealing process on the laser parameters. Therefore, care should be taken to determine the laser parameters, such as specific energy, required for laser sealing of a given material.

4. Clad layers of up to 1.5 mm thick were successfully produced although larger interaction times and higher power densities are required, compared with

sealing. Within the optimum processing range the clad layer was virtually crack free. The bonding to the substrate was satisfactory and there was little dilution.

Acknowledgements

We would like to thank Professor D. W. Pashley for providing laser laboratory facilities and Professor W. M. Steen of the University of Liverpool, for valuable discussions.

One of the authors (KMJ) thanks the ministry of Education and the Scientific Research Council, Baghdad, Iraq, and the Committee of Vice-Chancellors and Principals of the Universities of the United Kingdom for scholarship awards.

References

1. W. DRAPER *J. Metals*, **34** (6) (1982)24.
2. K. MOHAMMED JASIM, R. D. RAWLINGS and D. R. F. WEST, *J. Mater. Sci.* **25**(1990)4943.
3. W. M. STEEN, unpublished work, Imperial College, University of London (1986).
4. T. C. WELLS, *Surfacing J.* **9**(1978)2.
5. E. M. BREINAN, B. H. KEAR, L. E. GREANWALD and C. M. BANAS, in "Lasers in modern industry", edited by J. F. Ready, (Society of Manufacturing Engineers, MI USA, 1979) p. 147.
6. K. MOHAMMED JASIM, D. R. F. WEST and W. M. STEEN, *J. Mater. Sci. Lett* **7**(1988)1307.
7. K. MOHAMMED JASIM, D. R. F. WEST, W. M. STEEN and R. D. RAWLINGS, in "International Congress on Applications of Lasers and Electro-Optics (ICALEO'88), Laser Institute of America, USA, edited by J. Bruck (1989) p. 17.
8. K. MOHAMMED JASIM, D. R. F. WEST and R. D. RAWLINGS, in "Lasers in Industry (Laser-5)", edited by A. N. Lari and S. K. Ghosh, (IITT, Gournay-sur-Marne, France, 1989) p. 95.
9. K. MOHAMMED JASIM, D. R. F. WEST, W. M. STEEN and R. D. RAWLINGS, in "Laser Materials Processing III", edited by J. Mazumder and K. Mukherjee (TMS, USA, 1989) p. 55.
10. K. MOHAMMED JASIM, R. D. RAWLINGS, and D. R. F. WEST, *J. Mater. Sci.* **26**(1991)909.
11. *Idem*, unpublished work (1990).
12. D. L. RUCKLE, *Thin Solid Films* **73**(1980)455.
13. W. W. DULEY, in "Laser Surface Treatment of Metals", edited by C. W. Draper and P. Mazzoldi (Martinus Nijhoff, Dordrecht, The Netherlands, 1986) p. 3.

Received 7th May
and accepted 17th May 1991